Journal of Organometallic Chemistry, 428 (1992) 169–186
Elsevier Sequoia S.A., Lausanne
JOM 22312

Chemistry of hexaruthenium carbidocarbonyl cluster complexes. Syntheses and X-ray crystal structures of $Ru_6C(CO)_{15}(\mu\text{-SePh})(\mu\text{-AuPPh}_3)$, $Ru_6C(CO)_{14}(\mu\text{-SePh})_2$, and $Ru_6C(CO)_{14}(\mu\text{-SePh})(\mu,\eta^3\text{-}C_3H_5)$ *

Teiji Chihara and Hiroshi Yamazaki
Institute of Physical and Chemical Research (RIKEN), Wako-shi, Saitama 351-01 (Japan)

(Received July 26, 1991)

Abstract

Treatment of $[PPN]_2[Ru_6C(CO)_{16}]$ ($PPN = (PPh_3)_2N$) (**1**) with phenylselenenyl chloride at room temperature yields $[PPN][Ru_6C(CO)_{15}(SePh)]$ (**2a**). Reaction of **2a** with $AuClPPh_3$ in the presence of silver tetrafluoroborate affords $Ru_6C(CO)_{15}(SePh)(AuPPh_3)$ (**3**), which has edge bridging SePh and $AuPPh_3$ ligands. Heating of **2a** under reflux in bis(2-methoxyethyl) ether yields $Ru_6C(CO)_{14}(SePh)_2$ (**4**) with two edge bridging SePh ligands. Reaction of **2a** with allyl bromide at 110°C gives an allyl cluster $Ru_6C(CO)_{14}(SePh)(C_3H_5)$ (**5**) in which the allyl ligand coordinates to a metal-metal edge in a μ,η^3-manner and the SePh ligand bridges another edge. The structures of **3**, **4**, and **5** have been determined by single crystal X-ray diffraction studies.

Introduction

Many attempts to achieve cluster catalysis have been made with expectation of the multicenter transformation of small unsaturated molecules. However, homogeneous catalyses which are characteristic of metal clusters have scarcely been known [1]. This may be ascribed mostly to the facile degradation of the cluster framework under reaction conditions. In an attempt to overcome this problem and to achieve cluster catalysis, we have examined the reactions of hexaruthenium carbidocarbonyl clusters. It was expected that the encapsulated carbido atom may support the inherently weak metal–metal bonds from the inside of the metal skeleton without occupying coordination sites on the periphery [2]. We have already reported that the reactions of a dianionic cluster, $[PPN]_2[Ru_6C(CO)_{16}]$ ($PPN = (Ph_3P)_2N$) (**1**), with methyl iodide and allyl bromide afford methyl and allyl

---

Correspondence to: Dr. T. Chihara, Institute of Physical and Chemical Research (RIKEN), Wako-shi, Saitama 351-01, Japan.

* Dedicated to Professor Akio Yamamoto upon his retirement from Tokyo Institute of Technology and in honor of his contributions to organometallic chemistry.

derivatives, respectively [3], and that the reactions of the methyl derivative with carbon monoxide and dihydrogen give acetyl [3] and hydrido derivatives [4], respectively. In these cases the octahedral ruthenium metal skeleton was intact as expected even though the reaction conditions were fairly severe. We report here the preparation of the related hexaruthenium carbidocarbonyl clusters having phenyl selenide as an additional outer supporting ligand, which may have a function to open or block a coordination site on the periphery by changing the number of donating electrons.

Results and discussion

Reaction of $[PPN]_2[Ru_6C(CO)_{16}]$ (1) with phenylselenenyl chloride

The reaction of **1** with phenylselenenyl chloride proceeded quickly and was completed soon after the addition of phenylselenenyl chloride in CH_2Cl_2. Work-up of the reaction mixture afforded air-stable brown solids (**2a**). The IR spectrum showed a strong absorption at 1999 cm^{-1} in the $\nu(C{=}O)$ region. This may imply that **2a** is monoanionic, because the frequency shows an intermediate value between those of the dianion $[Et_4N]_2[Ru_6C(CO)_{16}]$ (1978 cm^{-1}) [5] and the neutral complex $Ru_6C(CO)_{17}$ (2064 and 2049 cm^{-1}) [6]. The related monoanionic complexes reveal a strong absorption band in the same range; $[Ru_6C(CO)_{16}(CH_3)]^-$ (2011 cm^{-1}) [3], $[Ru_6C(CO)_{15}(\mu,\eta^3\text{-}C_3H_5)]^-$ (1995 cm^{-1}) [3], $[Ru_6C(CO)_{16}(COCH_3)]^-$ (2013 cm^{-1}) [3], $[Ru_6C(CO)_{15}H]^-$ (2009 cm^{-1}) [4], and $[Ru_6C(CO)_{16}H]^-$ (2009 cm^{-1}) [4].

The $[Ph_3PMe]^+$ salt of the cluster (**2b**) was obtained in the same manner starting from $[Ph_3PMe]_2[Ru_6C(CO)_{16}]$. The ^1H NMR spectrum of **2b** showed multiplet peaks at τ 7.3–8.1 attributable to the phenyl protons of the SePh ligand and $[Ph_3PMe]$ cation and a doublet at τ 3.33 attributable to the methyl protons of the $[Ph_3PMe]$ cation with intensities in the ratio of 20:3. On the basis of these spectroscopic data, **2** was considered to be a monoanionic (phenylselenenyl) hexaruthenium carbidocarbonyl cluster. However, the number of the carbonyl ligands could not be deduced from the cluster electron counting rule [7], since the SePh ligand can be a 1, 3, or 5 electron donor. Elemental analysis failed to determine the exact formula, since it coincides with the calculated values for all possible clusters $[Ph_3PMe][Ru_6C(CO)_n(SePh)]$ (n = 14–16) within the experimental error. For the exact structure of **2**, it is desirable to undergo X-ray crystallographic analysis. However, all attempts to grow suitable crystals failed.

Synthesis of the (triphenylphosphine)gold derivative of 2

It is well known that the $[AuPPh_3]$ cation is isolobal with a proton [8] and forms adducts with anionic clusters in high yields without changing the cluster electron counting. Thus we tried to obtain a (triphenylphosphine)gold derivative of **2**.

Reaction of **2a** with chloro(triphenylphosphine)gold in the presence of silver tetrafluoroborate [9] followed by chromatography on silica gel afforded air-stable brown crystals. The IR spectrum showed a strong absorption at 2029 cm^{-1} in the $\nu(C{=}O)$ region indicating that the product is a neutral complex. Spectroscopic data and elemental analysis suggested that the product has the formula $Ru_6C(CO)_{15}(SePh)(AuPPh_3)$ (**3**).

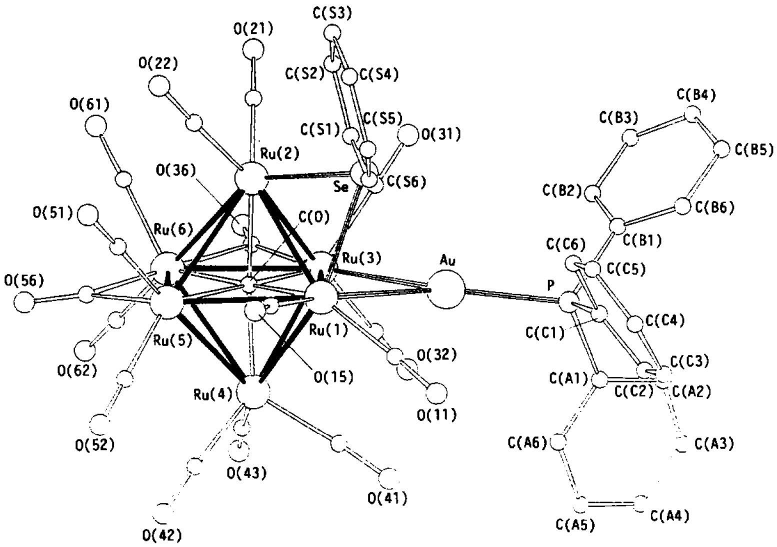

Fig. 1. The molecular structure of $Ru_6C(CO)_{15}(SePh)(AuPPh_3)$ (3) with the numbering of the oxygen atoms corresponding to that of the relevant carbonyl carbon atoms. The first digit of each oxygen number is the number of the ruthenium atom to which the carbonyl is attached.

In order to obtain the exact molecular structure, single-crystal X-ray analysis was undertaken. The structure is shown in Fig. 1. The selected interatomic distances and angles are presented in Tables 1 and 2, respectively. The octahedral metal geometry in **1** is kept unchanged in **3**. The metal–metal distances in **3** range from 2.7774(7) to 3.0812(7) Å. The shortest Ru(1)–Ru(2) edge corresponds to that bridged by the SePh ligand and the longest Ru(1)–Ru(3) edge corresponds to that

Table 1

Selected interatomic distances (Å) and esd values for $Ru_6C(CO)_{15}(SePh)(AuPPh_3)$ (3)

Ru(1)–Ru(2)	2.7774(7)	Ru(2)–Se	2.4669(8)
Ru(1)–Ru(3)	3.0812(7)	Ru(1)–Au	2.8515(6)
Ru(1)–Ru(4)	2.9226(9)	Ru(3)–Au	2.7253(6)
Ru(1)–Ru(5)	2.8808(8)	Ru(1)–C(11)	1.912(6)
Ru(2)–Ru(3)	2.8673(7)	Ru(1)–C(15)	1.902(6)
Ru(2)–Ru(5)	2.9676(8)	Ru(3)–C(36)	1.999(6)
Ru(2)–Ru(6)	2.9148(8)	Ru(5)–C(15)	2.627(7)
Ru(3)–Ru(4)	2.8361(8)	Ru(5)–C(56)	2.046(6)
Ru(3)–Ru(6)	2.8587(8)	Ru(6)–C(36)	2.298(6)
Ru(4)–Ru(5)	2.9488(8)	Ru(6)–C(56)	2.090(6)
Ru(4)–Ru(6)	2.9340(7)	Se–C(S1)	1.939(6)
Ru(5)–Ru(6)	2.8103(7)	Au–P	2.296(2)
Ru(1)–C(0)	2.036(5)	P–C(A1)	1.809(7)
Ru(2)–C(0)	2.024(6)	P–C(B1)	1.813(7)
Ru(3)–C(0)	2.054(5)	P–C(C1)	1.818(6)
Ru(4)–C(0)	2.047(6)	O(15)–C(15)	1.144(7)
Ru(5)–C(0)	2.087(5)	O(36)–C(36)	1.146(6)
Ru(6)–C(0)	2.054(5)	O(56)–C(56)	1.176(8)
Ru(1)–Se	2.4602(9)	O(62)–C(62)	1.134(10)

Table 2

Selected interatomic angles (deg) and esd values for $Ru_6C(CO)_{15}(SePh)(AuPPh_3)$ (3)

Ru(2)-Ru(1)-Se	55.80(2)	C(15)-Ru(5)-C(51)	84.7(2)
Ru(3)-Ru(1)-Au	54.53(2)	C(15)-Ru(5)-C(52)	87.9(3)
Ru(5)-Ru(1)-C(15)	62.8(2)	C(15)-Ru(5)-C(56)	177.2(2)
Se-Ru(1)-Au	74.52(2)	C(51)-Ru(5)-C(52)	83.7(3)
Se-Ru(1)-C(11)	105.8(2)	C(51)-Ru(5)-C(56)	93.9(2)
Se-Ru(1)-C(15)	99.6(2)	C(52)-Ru(5)-C(56)	94.4(3)
Au-Ru(1)-C(11)	71.0(2)	Ru(3)-Ru(6)-C(36)	44.0(1)
Au-Ru(1)-C(15)	155.4(2)	Ru(5)-Ru(6)-C(56)	46.5(1)
C(0)-Ru(1)-C(11)	146.0(3)	C(0)-Ru(6)-C(36)	89.8(2)
C(0)-Ru(1)-C(15)	108.9(2)	C(0)-Ru(6)-C(56)	94.2(2)
C(11)-Ru(1)-C(15)	88.3(3)	C(0)-Ru(6)-C(61)	126.3(3)
Ru(1)-Ru(2)-Se	55.57(2)	C(0)-Ru(6)-C(62)	139.8(3)
Se-Ru(2)-C(21)	106.1(2)	C(36)-Ru(6)-C(56)	175.3(3)
Se-Ru(2)-C(22)	98.0(2)	C(36)-Ru(6)-C(61)	87.4(2)
C(0)-Ru(2)-C(21)	129.8(2)	C(36)-Ru(6)-C(62)	86.8(3)
C(0)-Ru(2)-C(22)	130.0(2)	C(56)-Ru(6)-C(61)	92.4(2)
C(21)-Ru(2)-C(22)	87.8(2)	C(56)-Ru(6)-C(62)	88.5(3)
Ru(1)-Ru(3)-Au	58.44(2)	C(61)-Ru(6)-C(62)	93.6(3)
Ru(6)-Ru(3)-C(36)	52.9(2)	Ru(1)-Se-Ru(2)	68.62(3)
Au-Ru(3)-C(31)	76.4(2)	Ru(1)-Se-C(S1)	111.7(2)
Au-Ru(3)-C(32)	75.9(2)	Ru(2)-Se-C(S1)	113.0(2)
Au-Ru(3)-C(36)	162.9(2)	Ru(1)-Au-Ru(3)	67.03(2)
C(0)-Ru(3)-C(31)	128.9(3)	Ru(1)-Au-P	139.08(4)
C(0)-Ru(3)-C(32)	133.2(3)	Ru(3)-Au-P	153.83(4)
C(0)-Ru(3)-C(36)	98.7(2)	Au-P-C(A1)	111.1(2)
C(31)-Ru(3)-C(32)	95.8(3)	Au-P-C(B1)	113.2(2)
C(31)-Ru(3)-C(36)	90.8(3)	Au-P-C(C1)	113.3(2)
C(32)-Ru(3)-C(36)	93.1(3)	C(A1)-P-C(B1)	105.6(3)
C(0)-Ru(4)-C(41)	119.2(3)	C(A1)-P-C(C1)	106.5(3)
C(0)-Ru(4)-C(42)	127.1(3)	C(B1)-P-C(C1)	106.6(3)
C(0)-Ru(4)-C(43)	123.0(3)	Ru(1)-C(15)-Ru(5)	77.2(2)
C(41)-Ru(4)-C(42)	92.3(3)	Ru(1)-C(15)-O(15)	165.0(6)
C(41)-Ru(4)-C(43)	95.2(3)	Ru(5)-C(15)-O(15)	117.8(5)
C(42)-Ru(4)-C(43)	91.7(4)	Ru(3)-C(36)-Ru(6)	83.1(2)
Ru(1)-Ru(5)-C(15)	40.1(1)	Ru(3)-C(36)-O(36)	147.8(6)
Ru(6)-Ru(5)-C(56)	47.9(1)	Ru(6)-C(36)-O(36)	129.1(5)
C(0)-Ru(5)-C(15)	84.8(2)	Ru(5)-C(56)-Ru(6)	85.6(2)
C(0)-Ru(5)-C(51)	135.4(3)	Ru(5)-C(56)-O(56)	138.0(4)
C(0)-Ru(5)-C(52)	138.9(3)	Ru(6)-C(56)-O(56)	136.5(4)
C(0)-Ru(5)-C(56)	94.5(2)		

Table 3

Selected interatomic distances (Å) and esd values for $Ru_6C(CO)_{14}(SePh)_2$ (4)

Ru(1)-Ru(2)	2.8072(12)	Ru(1)-C(0)	2.0240(9)
Ru(1)-Ru(3)	2.8802(12)	Ru(2)-C(0)	2.038(8)
Ru(2)-Ru(3)	2.8971(15)	Ru(3)-C(0)	2.073(9)
Ru(1)-Ru(2)′	2.9147(12)	Ru(1)-Se	2.4378(14)
Ru(1)-Ru(3)′	2.9369(12)	Ru(2)-Se	2.4504(14)
Ru(2)-Ru(2)′	2.9735(13)	Se-C(1)	1.918(10)
Ru(3)-Ru(3)′	2.8564(13)		

Table 4

Selected interatomic angles (deg) and esd values for $Ru_6C(CO)_{14}(SePh)_2$ (4)

Ru(2)–Ru(1)–Se	55.16(4)	C(0)–Ru(2)–C(22)	129.0(4)
Se–Ru(1)–C(0)	100.43(18)	C(21)–Ru(2)–C(22)	88.4(5)
Se–Ru(1)–C(11)	101.3(3)	C(0)–Ru(3)–C(31)	124.7(4)
Se–Ru(1)–C(12)	96.5(3)	C(0)–Ru(3)–C(32)	117.6(3)
C(0)–Ru(1)–C(11)	123.4(4)	C(0)–Ru(3)–C(33)	124.3(4)
C(0)–Ru(1)–C(12)	133.6(4)	C(31)–Ru(3)–C(32)	93.5(4)
C(11)–Ru(1)–C(12)	94.5(5)	C(31)–Ru(3)–C(33)	92.0(5)
Ru(1)–Ru(2)–Se	54.74(4)	C(32)–Ru(3)–C(33)	97.3(5)
Se–Ru(2)–C(0)	99.61(7)	Ru(1)–Se–Ru(2)	70.10(4)
Se–Ru(2)–C(21)	102.0(3)	Ru(1)–Se–C(1)	112.0(3)
Se–Ru(2)–C(22)	101.5(3)	Ru(2)–Se–C(1)	115.2(3)
C(0)–Ru(2)–C(21)	131.1(4)		

bridged by the $AuPPh_3$ ligand. Such bond lengthening is a common effect in a cluster containing a μ-$AuPR_3$ unit [10].

The average metal–metal distance is 2.90(2) Å, which is similar to those of a series of hexaruthenium clusters such as $Ru_6C(CO)_{17}$ (2.903(17) Å) [11], $[PPN][Ru_6C(CO)_{16}(CH_3)]$ (2.903(14) Å) [3], $[Me_4N]_2[Ru_6C(CO)_{16}]$ (2.890(8) Å) [12], and $[Ph_4As]_2[Ru_6C(CO)_{16}]$ (2.89 Å) [13]. The difference in the negative charges on the clusters does not affect the metal–metal bond lengths appreciably. Consequently, the metal–carbide bond lengths in **3** (mean 2.050(9) Å) are almost the same as those in the case of the hexanuclear carbidocarbonyl clusters already reported.

The SePh ligand symmetrically bridges the shortest Ru(1)–Ru(2) edge with Ru–Se bond lengths to Ru(1) 2.4602(9) Å and to Ru(2) 2.4669(8) Å. The coordination around the Se atom is a very distorted tetrahedron (Ru(1)–Se–Ru(2) angle 68.62(3)°) with one coordination site occupied by the lone pair. These dimensions and coordination around the Se atom are similar to those of a dinuclear complex $Ru_2(\mu\text{-}SePh)_2(CO)_6$ (mean Ru–Se distance 2.520 Å, Ru–Se–Ru angle 64.8°) [14].

The $AuPPh_3$ ligand adopts asymmetric bridging mode at the longest Ru(1)–Ru(3) edge with Ru–Au distances 2.7253(6) and 2.8515(6) Å. This asymmetry of the bridging mode may be attributable to the less symmetry of the cluster molecule and similar values can be seen in $H_3Ru_4(CO)_{12}(AuPPh_3)$ (2.723(1) and 2.809(1) Å) [15], $Ru_5C(CO)_{15}(AuPPh_3)Cl$ (2.774(4) and 2.811(3) Å; 2.764(3) and 2.841(3) Å) [16], and $Ru_5C(CO)_{14}(AuPPh_3)Br$ (2.633(2) and 2.850(2) Å) [16]. More symmetrical AuP bridging bonds are found in the hexaruthenium carbidocarbonyl clusters $Ru_6C(CO)_{15}(NO)(AuPPh_3)$ (2.763(2) and 2.801(2) Å) [17] and $Ru_6C(CO)_{16}(AuPMePh_2)_2$ (2.758(1) and 2.788(1) Å) [18].

There are fifteen carbonyl ligands in **3** and three of them are bridging ligands. One carbonyl ligand, C(56)O(56), symmetrically bridges the Ru(5)–Ru(6) edge, with metal carbon bond lengths to Ru(5) 2.046(6) Å and to Ru(6) 2.090(6) Å. Another carbonyl ligand, C(36)O(36), asymmetrically bridges the Ru(3)–Ru(6) edge, with the shorter metal–carbon bond length (1.999(6) Å) to Ru(3) atom and the longer metal–carbon bond length (2.298(6) Å) to Ru(6) atom. The other carbonyl ligand, C(15)O(15), semi-bridges the Ru(1)–Ru(5) edge but highly asymmetrically (Ru(1)–C(15), 1.902(6) Å; Ru(5)–C(15), 2.627(7) Å; Ru(1)–C(15)–O(15), 165.0(6)°). These three bridging carbonyl ligands and bridging AuP ligand approximately lie on the least-squares plane Ru(1)–Ru(3)–Ru(5)–Ru(6)–C(0). The deviations of the Au, C(15), C(36), and C(56) atoms from the plane are −0.1934(7), 0.222(7), 0.139(7), and −0.144(6) Å, respectively.

The twelve remaining carbonyl ligands are terminal with Ru–C distances 1.868(7)–1.913(8) Å (average 1.893(4) Å), C–O distances 1.126(10)–1.152(9) Å (average 1.142(2) Å), and Ru–C–O angles higher than 175.3(7)° (Ru(4)–C(42)–O(42)).

Assuming that the SePh ligand serves as a three-electron donor and $AuPPh_3$ ligand formally a one-electron donor, **3** contains 86 cluster valence electrons; this number is in accord with the predictions of the PSEP approach [7]. Based on this structure, it seems probable that the starting monoanionic (phenylselenenyl)hexanuclear cluster (**2**) of unknown structure is $[Ru_6C(CO)_{15}(SePh)]^-$.

Formation of $Ru_6C(CO)_{14}(SePh)_2$ (4)

With expectation of the conversion of the three electron donating SePh ligand to the five electron donating one, the bis(2-methoxyethyl) ether solution of **2a** was heated under reflux for 1 h. Work-up of the reaction mixture afforded deep green crystals in a low yield. The IR spectrum shows a strong absorption at 2031 cm^{-1} suggesting that the product is a neutral hexanuclear ruthenium carbidocarbonyl cluster but not the one expected. In order to obtain the exact molecular structure, single-crystal X-ray analysis was undertaken. The formula of this cluster was revealed to be $Ru_6C(CO)_{14}(SePh)_2$ (**4**). The molecular structure is shown in Fig. 2 and the selected interatomic distances and angles are presented in Tables 3 and 4, respectively.

Cluster **4** has a crystallographic C_2 axis through the carbido atom C(0), the midpoint of the Ru(2)–Ru(2)′ bond, and the midpoint of the Ru(3)–Ru(3)′ bond. The six ruthenium atoms adopt a slightly distorted octahedron. The metal–metal distances (average 2.89(1) Å) in **4** are essentially the same as those in **3**. The shortest edges of this octahedron are Ru(1)–Ru(2) and Ru(1)′–Ru(2)′ (2.807(1) Å), on which each SePh ligand symmetrically bridges. The longest edge Ru(2)–Ru(2)′ (2.974(1) Å) is the adjacent of the shortest ones.

The two SePh ligands bridge over different edges and each Se atom constitutes a distorted tetrahedral configuration. Thus each SePh ligand formally donates three electrons to the cluster.

There are fourteen carbonyl ligands in **4**, and all of them are terminal: two for each SePh bridged Ru atom and three for each Ru atom without SePh ligand. The Ru–C distances lie in the range 1.852(10)–1.941(10) Å (average 1.892(7) Å), the C–O distances lie in the range 1.09(1)–1.16(1) Å (average 1.133(7) Å), and the Ru–C–O angles higher than 170(1)° (Ru(3)–C(32)–O(32) and Ru(3)′–C(32)′–O(32)′). Cluster **4** is stable with 86 overall valence electrons. It seems probable that **4** was produced by disproportionation of the SePh moiety of **2a**.

Preparation of $Ru_6C(CO)_{14}(SePh)(C_3H_5)$ (5)

A CH_2Cl_2 solution of **2** and allyl bromide was heated at 110°C in a pressure bottle. Work-up of the resulting solution afforded dark brown crystals. The IR spectrum showed a strong absorption at 2028 cm^{-1}, suggesting that the product was a neutral hexanuclear ruthenium cluster.

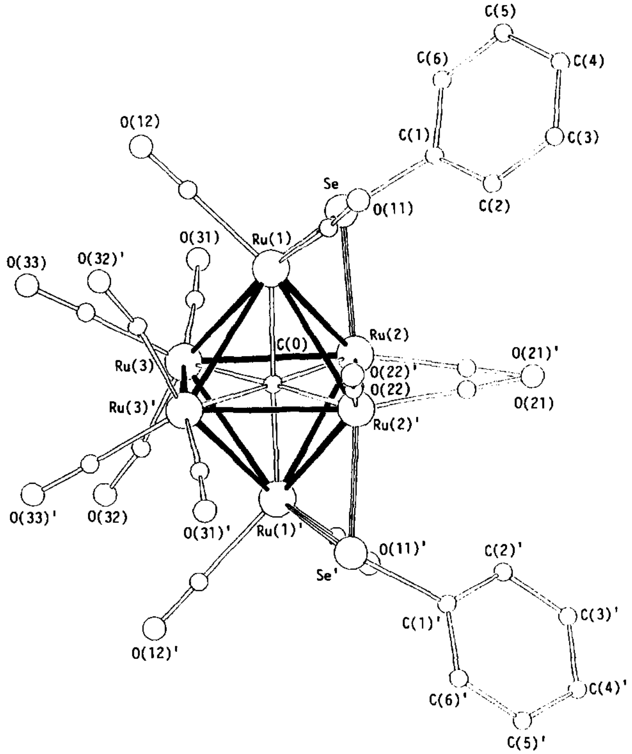

Fig. 2. The molecular structure of $Ru_6C(CO)_{14}(SePh)_2$ (4) showing the atom numbering scheme. Phenyl hydrogen atoms are omitted.

The ^1H NMR spectrum showed the presence of an allyl group. The 100 MHz ^1H NMR spectrum at 60°C showed a doublet at τ 4.36 ($J = 7.08$ Hz) attributable to the *syn*-hydrogens, a triplet of triplets at τ 2.35 ($J_{cis} = 7.08$ and $J_{trans} = 12.33$ Hz) attributable to the central hydrogen, and a doublet at τ 0.81 ($J = 12.33$ Hz) attributable to the *anti*-hydrogens. At room temperature the peak of *anti*-hydrogens became a broad peak at τ 0.5–1.2, while other peaks were intact. On cooling to −40°C all the allyl peaks became broad; *syn*-protons τ 4.3–4.6, central-proton 2.3–2.8, and *anti*-protons 0.4–0.7 and 1.0–1.3. These observations indicate the existence of some isomers in solution at low temperature and they exchange rapidly at high temperature. On the basis of these data and the elemental analysis, the complex was assumed to be an allyl hexanuclear carbidocarbonyl cluster $Ru_6C(CO)_{14}(SePh)(C_3H_5)$ (**5**).

In order to obtain the unequivocal structure of **5** the single-crystal X-ray analysis was undertaken. The structure is shown in Fig. 3. The selected interatomic distances and angles are presented in Tables 5 and 6, respectively.

The octahedral Ru_6C core of **2** is again retained in **5** and the six Ru atoms define a slightly distorted octahedron. The metal–metal distances range from 2.8241(8) (Ru(1)–Ru(2)) to 3.0039(8) Å (Ru(1)–Ru(5)) (mean 2.904(17) Å), and these values are almost the same as those in **1**, **3**, and **4**. The shortest edge is bridged by a SePh ligand as in the cases of **3** and **4**. The carbido atom lies at the center of the octahedron.

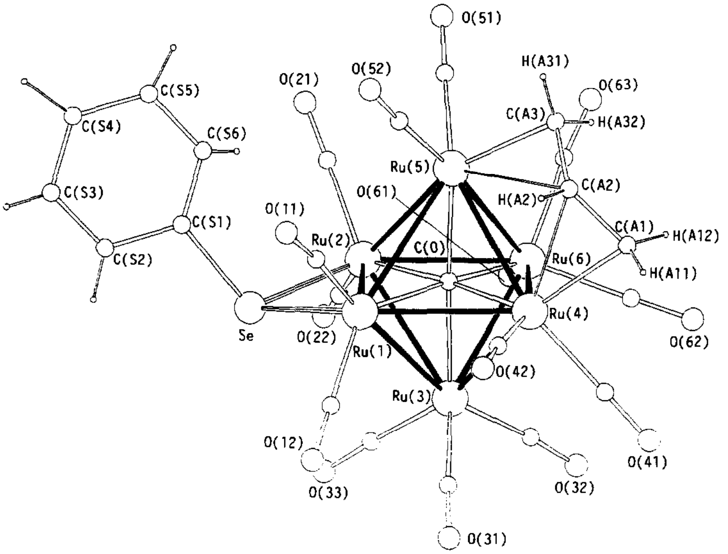

Fig. 3. The molecular structure of $Ru_6C(CO)_{14}(SePh)(C_3H_5)$ (**5**) showing the atom numbering scheme.

A bridging SePh ligand adopts a symmetric μ-bonding mode with Ru–Se distances 2.4218(9) and 2.4455(9) Å and formally donates three electrons to the cluster. The bonding mode and dimensions of the three SePh groups in **3**, **4**, and **5** are quite the same.

There is an allyl ligand bridging two Ru atoms different from the ones bridged by SePh ligand. The terminal carbon atoms C(A1) and C(A3) are bound to Ru(4) (2.207(6) Å) and Ru(5) (2.164(5) Å), respectively, and the central carbon atom C(A2) is bound to Ru(4) and Ru(5) with longer distances (2.447(6) and 2.722(5) Å). The central carbon atom C(A2) lies 0.171(7) Å above the least-squares plane

Table 5

Selected interatomic distances (Å) and esd values for $Ru_6C(CO)_{14}(SePh)(C_3H_5)$ (**5**)

Ru(1)–Ru(2)	2.8241(8)	Ru(5)–C(0)	2.055(5)
Ru(1)–Ru(3)	2.8672(11)	Ru(6)–C(0)	2.046(6)
Ru(1)–Ru(4)	2.9459(12)	Ru(1)–Se	2.4218(9)
Ru(1)–Ru(5)	3.0039(8)	Ru(2)–Se	2.4455(9)
Ru(2)–Ru(3)	2.9339(8)	Ru(4)–C(A1)	2.207(6)
Ru(2)–Ru(5)	2.9766(8)	Ru(4)–C(A2)	2.447(6)
Ru(2)–Ru(6)	2.8553(11)	Ru(5)–C(A2)	2.722(5)
Ru(3)–Ru(4)	2.8187(8)	Ru(5)–C(A3)	2.164(5)
Ru(3)–Ru(6)	2.8557(8)	Se–C(S1)	1.926(6)
Ru(4)–Ru(5)	2.8969(8)	C(A1)–C(A2)	1.420(9)
Ru(4)–Ru(6)	2.9374(8)	C(A2)–C(A3)	1.442(8)
Ru(5)–Ru(6)	2.9382(10)	C(A1)–H(A11)	0.90(5)
Ru(1)–C(0)	2.059(6)	C(A1)–H(A12)	0.96(7)
Ru(2)–C(0)	2.065(4)	C(A2)–H(A2)	0.97(7)
Ru(3)–C(0)	2.087(5)	C(A3)–H(A31)	0.97(6)
Ru(4)–C(0)	2.015(4)	C(A3)–H(A32)	1.05(8)

Table 6

Selected interatomic angles (deg) and esd values for $Ru_6C(CO)_{14}(SePh)(C_3H_5)$ (5)

Ru(2)-Ru(1)-Se	54.93(2)	C(51)-Ru(5)-C(52)	87.3(3)
Se-Ru(1)-C(0)	101.36(13)	C(51)-Ru(5)-C(A2)	119.3(2)
Se-Ru(1)-C(11)	97.3(2)	C(51)-Ru(5)-C(A3)	87.6(2)
Se-Ru(1)-C(12)	94.6(2)	C(52)-Ru(5)-C(A2)	86.5(2)
C(0)-Ru(1)-C(11)	132.5(2)	C(52)-Ru(5)-C(A3)	85.5(3)
C(0)-Ru(1)-C(12)	133.3(3)	C(A2)-Ru(5)-C(A3)	31.8(2)
C(11)-Ru(1)-C(12)	87.4(3)	C(0)-Ru(6)-C(61)	127.8(2)
Ru(1)-Ru(2)-Se	54.14(2)	C(0)-Ru(6)-C(62)	121.1(2)
Se-Ru(2)-C(0)	100.4(2)	C(0)-Ru(6)-C(63)	118.8(3)
Se-Ru(2)-C(21)	100.0(2)	C(61)-Ru(6)-C(62)	99.3(3)
Se-Ru(2)-C(22)	99.7(2)	C(61)-Ru(6)-C(63)	90.1(3)
C(0)-Ru(2)-C(21)	126.2(2)	C(62)-Ru(6)-C(63)	90.3(3)
C(0)-Ru(2)-C(22)	135.5(2)	Ru(1)-Se-Ru(2)	70.93(3)
C(21)-Ru(2)-C(22)	88.2(3)	Ru(1)-Se-C(S1)	110.7(2)
C(0)-Ru(3)-C(31)	124.9(3)	Ru(2)-Se-C(S1)	113.2(2)
C(0)-Ru(3)-C(32)	121.0(2)	Ru(4)-C(A1)-C(A2)	81.8(3)
C(0)-Ru(3)-C(33)	122.1(2)	Ru(4)-C(A1)-H(A11)	105(3)
C(31)-Ru(3)-C(32)	95.7(3)	Ru(4)-C(A1)-H(A12)	111(3)
C(31)-Ru(3)-C(33)	92.1(2)	C(A2)-C(A1)-H(A11)	121(4)
C(32)-Ru(3)-C(33)	92.9(3)	C(A2)-C(A1)-H(A12)	115(3)
Ru(5)-Ru(4)-C(A1)	90.9(2)	H(A11)-C(A1)-H(A12)	117(5)
Ru(5)-Ru(4)-C(A2)	60.5(1)	Ru(4)-C(A2)-Ru(5)	67.9(1)
C(0)-Ru(4)-C(41)	128.3(2)	Ru(4)-C(A2)-C(A1)	63.2(3)
C(0)-Ru(4)-C(42)	117.5(2)	Ru(4)-C(A2)-C(A3)	112.6(4)
C(0)-Ru(4)-C(A1)	131.7(2)	Ru(4)-C(A2)-H(A2)	109(4)
C(0)-Ru(4)-C(A2)	105.6(2)	Ru(5)-C(A2)-C(A1)	121.6(4)
C(41)-Ru(4)-C(42)	91.0(3)	Ru(5)-C(A2)-C(A3)	52.3(3)
C(41)-Ru(4)-C(A1)	83.4(2)	Ru(5)-C(A2)-H(A2)	101(3)
C(41)-Ru(4)-C(A2)	118.2(2)	C(A1)-C(A2)-C(A3)	125.0(7)
C(42)-Ru(4)-C(A1)	93.5(2)	C(A1)-C(A2)-H(A2)	124(3)
C(42)-Ru(4)-C(A2)	88.5(3)	C(A3)-C(A2)-H(A2)	110(3)
C(A1)-Ru(4)-C(A2)	35.0(2)	Ru(5)-C(A3)-C(A2)	95.9(4)
Ru(4)-Ru(5)-C(A2)	51.5(1)	Ru(5)-C(A3)-H(A31)	107(3)
Ru(4)-Ru(5)-C(A3)	79.5(2)	Ru(5)-C(A3)-H(A32)	109(4)
C(0)-Ru(5)-C(51)	132.3(3)	C(A2)-C(A3)-H(A31)	121(4)
C(0)-Ru(5)-C(52)	129.2(3)	C(A2)-C(A3)-H(A32)	116(3)
C(0)-Ru(5)-C(A2)	95.5(2)	H(A31)-C(A3)-H(A32)	106(5)
C(0)-Ru(5)-C(A3)	120.3(2)		

Ru(2)-Ru(3)-Ru(4)-Ru(5)-C(0), and the terminal carbon atoms C(1) and C(3) lie 0.842(7) and 0.800(7) Å above the plane, respectively. The dihedral angle between the least-squares plane and the allyl plane defined by atoms C(A1)-C(A2)-C(A3) is 79.6(7)°. All the hydrogen atoms lie above the allyl plane away from the Ru atoms. Central, H(2), and two *anti*-hydrogen atoms, H(12) and H(32), lie 0.22(6), 0.14(6), and 0.14(6) Å above the allyl plane, respectively, and *syn*-hydrogens, H(11) and H(31), lie 0.30(5) and 0.53(6) Å above the plane, respectively. Thus the allyl ligand adopts quite the same μ,η^3-bonding mode as those of $[PPN][Ru_6C(CO)_{15}(C_3H_5)]$ [3], $Ru_3(CO)_8(C_3H_5)(P(Ph)CH_2PPh_2)$ [19], and $Os_3(CO)_{10}(C_3H_5)(AuPEt_3)$ [20].

There are fourteen terminal carbonyl ligands in 5, two for each of the SePh or C_3H_5 bridged Ru atom and three for each of the non-bridged Ru atom. The

Ru–C–O angles are higher than 173.3(8)° (Ru(6)–C(63)–O(63)), the Ru–C distances range from 1.852(9) to 1.923(6) Å (mean 1.892(6) Å), and C–O distances range from 1.130(11) to 1.160(9) Å (mean 1.139(2) Å). These dimensions are almost the same as those in **3** and **4**. Cluster **5** has 86 valence electrons and is electronically saturated.

Experimental

Chloro(triphenylphosphine)gold [21] and $[PPN]_2[Ru_6C(CO)_{16}]$ (**1**) [5] were prepared according to the reported methods. Phenylselenenyl chloride, silver tetrafluoroborate, and allyl bromide were commercially available and used as received. All the reactions and subsequent procedures were carried out under argon. IR and ^1H NMR spectra were recorded on a Jasco A-202 spectrophotometer and a Jeol FX-100 spectrometer, respectively.

*Preparation of [PPN][Ru₆C(CO)₁₅(SePh)] (**2a**)*

To a CH_2Cl_2 solution (10 mL) of cluster **1** (542 mg, 0.253 mmol), a CH_2Cl_2 solution (2 mL) of phenylselenenyl chloride (100 mg, 0.52 mmol) was carefully added with vigorous stirring until the silica gel TLC spot due to **1** had just disappeared (approx. 1.3 mL). After completion of the addition, the solvent was removed under reduced pressure. The residue was dissolved in a minimum quantity (approx. 2 mL) of CH_2Cl_2 and applied to an alumina (5% water) column chromatography. Elution with a benzene/CH_2Cl_2 (1:1) mixture separated a reddish brown band. Evaporation of the eluate to dryness gave air-stable brown solids of **2a** (263 mg, 0.152 mmol, 60%). IR(CH_2Cl_2): ν(C=O) 2058m, 1999s, 1986w(sh), 1949w(sh), and 1802m(br) cm^{-1}. ^1H NMR (acetone-d_6): τ 7.3–7.9 (m, phenyl protons).

By the same procedure $[Ph_3PMe][Ru_6C(CO)_{15}(SePh)]$ (**2b**) (72 mg, 55% yield) was obtained from $[Ph_3PMe]_2[Ru_6C(CO)_{16}]$ (153 mg). ^1H NMR (acetone-d_6): τ 7.3–8.1 (20H, m, Ph_3P and PhSe) and 3.33 (3H, d, J(H–P) = 14.0 Hz, Me). Anal. Found: C, 33.50; H, 1.57. $C_{41}H_{23}O_{15}PRu_6Se$ calc.: C, 33.46; H, 1.57%.

Preparation of Ru₆C(CO)₁₅(SePh)(AuPPh₃) (3)

Cluster **2a** (286 mg, 0.165 mmol) and chloro(triphenylphosphine)gold (82 mg, 0.165 mmol) were dissolved in CH_2Cl_2 (10 mL) and an acetone solution (3 mL) of silver tetrafluoroborate (32 mg, 0.165 mmol) was added under stirring. After 10 min the solvent was removed under reduced pressure, and the residue was subjected to silica gel (3% water) column chromatography. Elution with a hexane/benzene (1:1) solvent mixture separated a brown band, and the eluate was evaporated to dryness. The residue was crystallized from CH_2Cl_2/ethanol to give brown crystals of $Ru_6C(CO)_{15}(SePh)(AuPPh_3) \cdot C_2H_5OH$ (182 mg, 0.107 mmol, 65%). IR (CH_2Cl_2): ν(C=O) 2073s, 2029vs, 2001w(sh), 1986w, 1858m(br), and 1835m(br) cm^{-1}. ^1H NMR (acetone-d_6): τ 7.3–7.9 (m, phenyl). Anal. Found: C, 29.54; H, 1.33. $C_{40}H_{20}AuO_{15}PRu_6Se \cdot C_2H_5OH$ calc.: C, 29.67; H, 1.54%.

Preparation of Ru₆C(CO)₁₄(SePh)₂ (4)

Cluster **2a** (500 mg) was dissolved in bis(2-methoxyethyl) ether (5 mL) and the solution was refluxed for 1 h. The solvent was removed under reduced pressure, and the residue was subjected to an alumina (5% water) column chromatography. The first green band was eluted with hexane/benzene (1:1), and the eluate was evaporated to dryness. The residue was crystallized from benzene/hexane by diffusion to give deep green crystals of **4** (13.5 mg). IR (CH_2Cl_2): ν(C=O) 2076m, 2031s, 2008w(sh), 1976w(sh), and 1843w(br) cm^{-1}. ^1H NMR (acetone-d_6): τ 7.3–7.6 (m, phenyl). Anal. Found: C, 24.89; H, 0.81. $C_{27}H_{10}O_{14}Ru_6Se_2$ calc.: C, 24.51, H, 0.76%.

From the second reddish-brown band eluted with a benzene/CH_2Cl_2 (1:1) mixture, **2a** was recovered (115 mg, 23% recovery).

Preparation of $Ru_6C(CO)_{14}(SePh)(C_3H_5)$ (5)

A CH_2Cl_2 (2 mL) solution of cluster **2a** (181 mg, 0.104 mmol) and allyl bromide (0.2 mL) was placed in a stainless steel pressure vessel equipped with an inner glass tube, and heated at 110°C for 1 h. The solution was subjected to silica gel (3% water) column chromatography (1.8 cm i.d. × 50 cm). A dark brown band was eluted with hexane/benzene (20:1–10:1 v/v), and the eluate was evaporated to dryness. Crystallization of the residue from CH_2Cl_2/methanol at −20°C yielded dark brown crystals of $Ru_6C(CO)_{14}(SePh)(C_3H_5)\cdot CH_2Cl_2$. The crystals were washed with a minimum amount of methanol (0.5 mL × 2) and dried under reduced pressure (42.8 mg, 0.033 mmol, 32%). IR (CH_2Cl_2): ν(C=O) 2076m, 2035w(sh), 2028s, 1974w(sh), and 1845w(br) cm^{-1}. ^1H NMR (acetone-d_6, 60°C): τ 7.3–7.5 (5H, m, phenyl), 4.36 (2H, d, $J = 7.08$ Hz, *syn*-H), 2.35 (1H, tt, $J = 12.33$ and 7.08 Hz, central-H), and 0.81 (2H, d, $J = 12.33$ Hz, *anti*-H). Anal. Found: C, 23.98; H, 0.89. $C_{24}H_{10}O_{14}Ru_6Se$ calc.: C, 23.87; H, 0.83%.

Structure determination

Data collection. Brown single crystals of **3** for X-ray measurements were obtained by diffusion of hexane to a benzene solution of **3** in a glass tube (8 mm i.d.) at room temperature. Deep green single crystals of **4** were obtained by addition of hexane to a benzene solution of **4** in a flash at room temperature. They were fixed with Apiezon grease L in a glass capillary which was filled with argon. Dark brown single crystals of **5** were obtained by addition of methanol to a CH_2Cl_2 solution of **5** at −20°C. The single crystal of **5** was fixed with the mother liquor in a glass capillary which was filled with argon.

Measurements were carried out at 21°C for **3** and **4**. For **5**, measurements were made at −20°C, since partial dissolution of the crystal occurred at room temperature during measurements. Unit cell dimensions were derived from the least-squares fit of the angular settings of 25 reflections with $20° < 2\theta < 25°$. Intensity data were collected using an Enraf-Nonius CAD4 four-circle automated diffractometer with graphite-monochromatized Mo-K_α radiation. Crystal data and experimental details are given in Table 7.

Structure analysis and refinement for 3. A survey of the data set revealed no systematic extinctions and no symmetry other than the Friedel condition ($\bar{1}$). Thus the crystal belongs to the triclinic class with space group $P1$ or $P\bar{1}$. The latter centrosymmetric possibility was strongly indicated by the cell volume (consistent with $Z = 2$) and was confirmed by the successful solution of the structure in this higher symmetry space group. Data were corrected for absorption by interpolation in ϕ and 2θ between a set of normalized transmission curves based upon ψ scans

Table 7

Crystal data and refinement details

	$Ru_6C(CO)_{14}$- $(SePh)(AuPPh_3)$ (3)	$Ru_6C(CO)_{14}$- $(SePh)_2$ (4)	$Ru_6C(CO)_{14}$- $(SePh)(C_3H_5)$ (5)
formula	$C_{40}H_{20}AuO_{15}PRu_6Se$ $\cdot C_6H_6$	$C_{27}H_{10}O_{14}$-Ru_6Se_2	$C_{24}H_{10}O_{14}Ru_6Se$ $\cdot CH_2Cl_2$
F.W.	1732.0	1322.7	1292.6
crystal system	triclinic	orthorhombic	monoclinic
space group (No.)	$P\bar{1}$ (2)	$P2_12_12$ (18)	$P2_1/n$ (14)
a, Å	14.776(2)	9.833(3)	20.365(4)
b, Å	19.133(2)	15.996(4)	10.546(2)
c, Å	10.201(1)	10.695(3)	17.483(6)
α, deg	90.28(1)	90	90
β, deg	108.13(1)	90	114.97(2)
γ, deg	72.26(1)	90	90
cell volume, $Å^3$	2597	1682	3404
Z	2	2	4
D_{calcd}, g cm^{-3}	2.21	2.61	2.52
systematic absences	no	$h00$, h odd $0k0$, k odd	$h0l$, $h+l$ odd $0k0$, k odd
temperature, °C	21	21	−20
crystal size, mm	0.12 × 0.21 × 0.58	0.22 × 0.30 × 0.40	0.16 × 0.23 × 0.62
λ(Mo-K_α), Å	0.71073	0.71073	0.71073
2θ limit, deg	55	55	55
scan method	ω	ω	ω
scan range (ω), deg	$0.8+0.35 \tan\theta$	$1.2+0.35 \tan\theta$	$0.8+0.35 \tan\theta$
scan rate (ω), deg min^{-1}	4.12 + variable	4.12 + variable	4.12 + variable
collection region	$\pm h, \pm k, l$	$+h, +k, +l$	$\pm h, +k, +l$
unique obsd reflections	10370	2395	6759
criterion for obsd F	$\geq 3\sigma$	$\geq 3\sigma$	$\geq 3\sigma$
no. of parameters	632	243	482
data/parameters	16.4	9.87	14.0
linear abs coeff μ, cm^{-1}	52.61	47.69	38.06
$F(000)$, e	1628	1232	2424
correction applied	Lz	Lz	Lz
correction made	North-Phillips	no	North-Phillips
transmission coeff.	0.656–0.999		0.594–0.998
decay	negligible	negligible	negligible
R, R_w	0.034, 0.032 [a]	0.041, 0.034 [b]	0.032, 0.030 [a]
GOF [c]	2.50	2.41	2.90
mean shift/esd max, final cycle	0.70	0.48	0.47
$\delta\rho_{map}$, e $Å^{-3}$	1.40	1.62	0.88

[a] $w = 1/\sigma(F_o)$. [b] $w = 1/\sigma^2(F_o)$. [c] $[\Sigma w(F_o - F_c)^2/(N_{obsd} - N_{param})]^{1/2}$.

of close-to-axial reflections [22]. Throughout the analysis, the analytical form of the scattering factor [23a] for the appropriate neutral atom used in calculating F_c was corrected for both real ($\Delta f'$) and imaginary ($\Delta f''$) components of anomalous dispersions [23b].

The structure was solved by direct methods using the program MULTAN [24], which located six ruthenium atoms. The remaining non-hydrogen atoms were

Table 8

Atomic coordinates and equivalent temperature factors (Å^2) for $Ru_6C(CO)_{15}(SePh)(AuPPh_3)$ (3) with esd values in parentheses

Atom	x	y	z	B_{eq} [a]
Ru(1)	0.24997(3)	0.35185(2)	0.61959(4)	2.8
Ru(2)	0.36245(3)	0.32774(2)	0.89939(4)	2.6
Ru(3)	0.45840(3)	0.23351(2)	0.72913(5)	2.9
Ru(4)	0.42383(4)	0.35659(3)	0.54513(5)	3.2
Ru(5)	0.34614(3)	0.45952(2)	0.73021(5)	2.8
Ru(6)	0.53359(3)	0.34964(2)	0.84150(5)	2.9
Se	0.20967(4)	0.29256(3)	0.79782(6)	3.1
Au	0.29368(2)	0.20017(1)	0.57083(3)	3.9
P	0.21269(12)	0.12243(9)	0.45245(18)	3.7
O(11)	0.10082(43)	0.34193(32)	0.34137(51)	7.5
O(15)	0.09847(33)	0.50292(25)	0.59311(57)	6.2
O(21)	0.48927(38)	0.22176(28)	1.15566(49)	6.2
O(22)	0.28980(37)	0.43342(25)	1.09350(48)	5.4
O(31)	0.45416(38)	0.10803(25)	0.90658(51)	5.7
O(32)	0.53382(46)	0.13561(32)	0.52266(62)	8.1
O(36)	0.67637(33)	0.18513(25)	0.91282(57)	6.3
O(41)	0.31243(43)	0.30295(30)	0.28184(47)	6.4
O(42)	0.40066(53)	0.49642(30)	0.38153(59)	8.4
O(43)	0.62639(42)	0.28166(37)	0.50878(68)	8.7
O(51)	0.24736(37)	0.56621(25)	0.90155(52)	5.7
O(52)	0.28182(46)	0.59724(27)	0.53971(55)	7.3
O(56)	0.52511(30)	0.51034(22)	0.86700(45)	4.2
O(61)	0.62103(34)	0.33430(26)	1.15656(44)	5.2
O(62)	0.72767(36)	0.35546(32)	0.80330(62)	7.0
C(0)	0.39444(38)	0.34529(28)	0.72578(53)	2.7
C(11)	0.15771(50)	0.34309(37)	0.44605(64)	4.6
C(15)	0.16545(46)	0.45029(34)	0.61139(64)	4.2
C(21)	0.44042(43)	0.26168(33)	1.05810(61)	3.8
C(22)	0.31496(43)	0.39537(31)	1.01640(59)	3.5
C(31)	0.45387(44)	0.15631(32)	0.83930(64)	3.8
C(32)	0.50497(51)	0.17260(36)	0.59975(70)	4.7
C(36)	0.59760(45)	0.22350(34)	0.85215(68)	4.2
C(41)	0.35156(51)	0.32321(37)	0.38350(63)	4.5
C(42)	0.40809(60)	0.44626(39)	0.44645(72)	5.3
C(43)	0.55118(55)	0.31131(45)	0.52569(78)	5.7
C(51)	0.28555(43)	0.52457(32)	0.83960(60)	3.5
C(52)	0.30780(49)	0.54488(34)	0.61120(66)	4.4
C(56)	0.48677(40)	0.46474(30)	0.83176(56)	3.2
C(61)	0.58724(42)	0.33961(32)	1.03771(63)	3.8
C(62)	0.65572(45)	0.35258(35)	0.81740(70)	4.3
C(S1)	0.09358(40)	0.35690(35)	0.83741(63)	3.8
C(S2)	0.09331(53)	0.35490(45)	0.97219(71)	5.6
C(S3)	0.00230(58)	0.39409(53)	0.99860(84)	7.1
C(S4)	0.08080(56)	0.43309(49)	0.89068(90)	6.9
C(S5)	0.07903(53)	0.43468(48)	0.75545(90)	6.7
C(S6)	0.00892(48)	0.39571(43)	0.72727(77)	5.5
C(A1)	0.25916(45)	0.08891(33)	0.31197(64)	4.0
C(A2)	0.27372(68)	0.01708(40)	0.27694(88)	6.7
C(A3)	0.31072(79)	−0.00380(45)	0.16492(100)	8.2
C(A4)	0.33413(72)	0.04411(51)	0.09379(102)	8.0
C(A5)	0.31763(82)	0.11449(55)	0.12388(101)	8.7
C(A6)	0.28101(72)	0.13835(47)	0.23520(86)	7.1

Table 8 (continued)

Atom	x	y	z	B_{eq} ^{a}
C(B1)	0.23084(49)	0.04073(33)	0.55952(68)	4.3
C(B2)	0.32301(59)	0.00805(40)	0.65776(81)	6.2
C(B3)	0.34212(72)	−0.05691(46)	0.73738(93)	7.9
C(B4)	0.26939(80)	−0.08884(51)	0.71883(102)	9.1
C(B5)	0.17549(75)	−0.05901(54)	0.61570(115)	9.4
C(B6)	0.15444(65)	0.00895(48)	0.53363(104)	7.9
C(C1)	0.07779(47)	0.16598(36)	0.37560(76)	4.9
C(C2)	0.02834(59)	0.16240(53)	0.23571(87)	7.5
C(C3)	−0.08016(76)	0.20141(63)	0.18687(107)	10.2
C(C4)	−0.12420(69)	0.23936(57)	0.27903(110)	9.2
C(C5)	−0.07626(71)	0.24122(56)	0.41359(116)	9.2
C(C6)	0.02794(59)	0.20418(45)	0.46519(103)	7.3
C(D1)	0.06526(89)	0.08093(68)	−0.15220(134)	12.3
C(D2)	0.05227(89)	0.15443(70)	−0.14408(134)	12.1
C(D3)	−0.03210(87)	0.20628(69)	−0.18379(131)	11.9
C(D4)	−0.11757(98)	0.19297(71)	−0.25185(148)	13.4
C(D5)	−0.11833(93)	0.12214(71)	−0.24499(162)	14.7
C(D6)	−0.02774(116)	0.06343(75)	−0.16928(165)	16.2

^{a} $B_{eq} = \frac{4}{3}(\Sigma_i \Sigma_j B_{ij} a_i b_j)$.

located from subsequent difference Fourier syntheses. They were refined by the block-diagonal least-squares method [25], with anisotropic thermal parameters for all the atoms. The final $R(F)$ and $R_w(F)$ values are 0.034 and 0.032 with the weighting scheme $w = 1/\sigma$. The final difference Fourier synthesis showed no unexpected features, with the highest peak (1.4 e Å^{-3}) within the covalent radius of the ruthenium atom. Cluster **3** crystallized with one molecule of benzene in the asymmetric crystal unit. The final positional and thermal parameters are listed in Table 8.

Structure analysis and refinement for 4. A survey of the data set revealed the symmetry of the reciprocal lattice (*mmm*) indicating an orthorhombic system and the systematic absences $h00$ for $h = 2n + 1$ and $0k0$ for $k = 2n + 1$, compatible only with space group $P2_12_12$ (no. 18). Data were not corrected for absorption, because deviations of F_o for axial reflections at χ 90° were within ±5%. The structure was solved by direct methods using MULTAN, which located three ruthenium atoms. The remaining non-hydrogen atoms and five hydrogen atoms were located from subsequent difference Fourier syntheses. They were refined by the block-diagonal least-squares method, with anisotropic thermal parameters for all non-hydrogen atoms and isotropic thermal parameter for hydrogen atoms. The final R and R_w values are 0.041 and 0.034 with the weighting scheme $w = 1/\sigma^2$. The final difference Fourier synthesis showed noisy but uninformative backgrounds. The maximum peak (1.62 e Å^{-3}) was located within the covalent radius of the ruthenium atom. Cluster **4** has a crystallographic C_2 axis throughout the molecule. Final atomic coordinates and thermal parameters are presented in Table 9.

Structure analysis and refinement for 5. A survey of the data set revealed the symmetry of the reciprocal lattice ($2/m$) indicating a monoclinic system and the systematic extinctions $h0l$ for $h + l = 2n + 1$ and $0k0$ for $k = 2n + 1$; the cen-

Table 9

Atomic coordinates and equivalent temperature factors (Å^2) for $Ru_6C(CO)_{14}(SePh)_2$ (**4**) with esd values in parentheses

Atom	x	y	z	B_{eq} [a]
Ru(1)	0.20160(8)	0.97498(5)	0.08848(8)	2.1
Ru(2)	−0.02230(8)	0.90816(5)	0.21648(7)	2.1
Ru(3)	−0.02466(8)	0.91210(5)	−0.05382(7)	2.3
Se	0.20265(11)	0.84320(6)	0.20243(10)	2.5
O(11)	0.41084(80)	1.07552(49)	0.22923(87)	5.3
O(12)	0.40339(80)	0.92332(49)	−0.11034(90)	5.5
O(21)	−0.07083(102)	0.91463(55)	0.49557(72)	5.7
O(22)	−0.20810(88)	0.75906(45)	0.21162(83)	5.2
O(31)	0.01986(110)	0.72583(48)	−0.02560(77)	6.0
O(32)	−0.29599(82)	0.88848(51)	−0.18258(86)	5.8
O(33)	0.13093(92)	0.91284(59)	−0.29637(78)	6.2
C(0)	0.0	1.0	0.08639(111)	1.5
C(11)	0.32801(110)	1.03733(70)	0.18022(112)	4.0
C(12)	0.33109(105)	0.94195(64)	−0.03899(97)	3.0
C(21)	−0.04927(115)	0.91376(67)	0.39166(95)	3.6
C(22)	−0.13488(111)	0.81547(61)	0.21330(104)	3.3
C(31)	−0.00124(109)	0.79462(63)	−0.03278(93)	3.0
C(32)	−0.19852(114)	0.90061(62)	−0.12401(113)	3.7
C(33)	0.07484(104)	0.91154(73)	−0.20509(111)	3.8
C(1)	0.31040(108)	0.84940(63)	0.35131(94)	2.9
C(2)	0.30455(114)	0.91440(77)	0.44071(102)	4.1
C(3)	0.39285(120)	0.91403(98)	0.54157(100)	5.1
C(4)	0.48430(142)	0.85175(94)	0.55373(101)	5.8
C(5)	0.49268(150)	0.78934(83)	0.46513(118)	6.0
C(6)	0.40425(133)	0.78671(72)	0.36706(111)	4.3
H(2)	0.2003(129)	0.9244(73)	0.4578(106)	9.8(4.2) [b]
H(3)	0.3236(138)	0.9542(77)	0.5877(120)	11.3(4.4) [b]
H(4)	0.5635(104)	0.8614(66)	0.6328(92)	6.1(3.1) [b]
H(5)	0.5236(134)	0.7455(95)	0.4851(120)	9.9(3.9) [b]
H(6)	0.3900(89)	0.7293(54)	0.3130(82)	3.9(2.5) [b]

[a] $B_{eq} = \frac{4}{3}(\Sigma_i \Sigma_j B_{ij} a_i b_j)$ for non-hydrogen atoms. [b] Refined isotropically.

trosymmetric monoclinic space group $P2_1/n$ was obtained. Data were corrected for absorption. The structure was solved by direct methods using MULTAN, which located six ruthenium atoms of the asymmetric unit. Subsequent difference Fourier syntheses revealed the positions of all non-hydrogen atoms and twelve hydrogen atoms. All the non-hydrogen atoms were refined with anisotropic thermal parameters and all the hydrogen atoms were refined with isotropic thermal parameters. The final model converged with $R = 0.032$ and $R_w = 0.030$ with the weighting scheme $w = 1/\sigma$. The final difference Fourier synthesis showed no unexpected features, with the highest peak (0.88 e Å^{-3}) within a covalent radius of the ruthenium atom. Cluster **5** crystallized with a molecule of CH_2Cl_2 in the asymmetric crystal unit. Final positional and thermal parameters are listed in Table 10. Complete tables of bond lengths and angles, lists of thermal parameters, and observed and calculated structure factors are available from the authors.

Table 10

Atomic coordinates and equivalent temperature factors (Å^2) for Ru$_6$C(CO)$_{14}$(SePh)(C$_3$H$_5$) (**5**) with esd values in parentheses

Atom	x	y	z	B_{eq} [a]
Ru(1)	0.21053(2)	0.14340(4)	0.39985(3)	2.1
Ru(2)	0.08579(2)	0.26282(4)	0.39813(2)	2.0
Ru(3)	0.16645(2)	0.07897(4)	0.53056(3)	2.0
Ru(4)	0.29354(2)	0.22438(4)	0.57603(3)	2.1
Ru(5)	0.22018(2)	0.41718(4)	0.45090(3)	2.4
Ru(6)	0.16028(2)	0.34018(4)	0.57006(3)	2.1
Se	0.08892(3)	0.11821(5)	0.29037(3)	2.5
O(11)	0.28437(32)	0.19776(56)	0.28545(36)	6.5
O(12)	0.25227(28)	−0.12919(46)	0.39166(32)	5.0
O(21)	0.01409(26)	0.48764(46)	0.28956(31)	5.0
O(22)	−0.06188(22)	0.19631(46)	0.38875(31)	4.4
O(31)	0.25589(25)	−0.16361(42)	0.56606(30)	4.4
O(32)	0.14516(28)	0.05961(47)	0.69250(27)	4.7
O(33)	0.02914(23)	−0.06872(44)	0.43113(28)	4.3
O(41)	0.34583(25)	0.08162(49)	0.74242(27)	4.6
O(42)	0.40005(25)	0.07553(54)	0.53343(33)	5.7
O(51)	0.14261(26)	0.66797(44)	0.39729(32)	5.1
O(52)	0.28505(32)	0.46840(56)	0.32856(35)	6.4
O(61)	0.01022(24)	0.35302(52)	0.56987(32)	5.1
O(62)	0.24856(27)	0.32773(50)	0.76060(26)	4.9
O(63)	0.16569(31)	0.62736(44)	0.58494(35)	5.6
C(0)	0.19153(26)	0.24876(48)	0.48761(31)	2.0
C(11)	0.25647(35)	0.18193(62)	0.32843(41)	3.6
C(12)	0.23687(31)	−0.02623(59)	0.39626(38)	3.2
C(21)	0.04351(31)	0.40369(57)	0.33167(35)	3.0
C(22)	−0.00596(29)	0.22134(53)	0.39335(34)	2.7
C(31)	0.22273(30)	−0.07331(57)	0.55198(36)	3.0
C(32)	0.15312(30)	0.07307(56)	0.63278(35)	2.9
C(33)	0.07922(31)	−0.00982(55)	0.46841(34)	2.9
C(41)	0.32500(30)	0.13567(57)	0.67998(36)	3.0
C(42)	0.35660(31)	0.13169(61)	0.54599(38)	3.4
C(51)	0.17091(32)	0.57309(60)	0.41560(38)	3.5
C(52)	0.25907(36)	0.44577(65)	0.37391(42)	4.0
C(61)	0.06532(32)	0.34520(62)	0.56847(38)	3.5
C(62)	0.21750(32)	0.33054(62)	0.68954(38)	3.4
C(63)	0.16488(36)	0.52081(59)	0.57541(42)	3.7
C(S1)	0.07882(28)	0.20344(56)	0.18860(32)	2.6
C(S2)	0.05148(34)	0.13134(62)	0.11647(35)	3.5
C(S3)	0.04112(40)	0.18656(77)	0.04035(39)	4.8
C(S4)	0.05840(38)	0.31141(78)	0.03656(40)	4.6
C(S5)	0.08560(38)	0.38335(70)	0.10860(40)	4.2
C(S6)	0.09683(35)	0.32965(64)	0.18502(37)	3.7
C(A1)	0.37767(30)	0.36156(62)	0.65193(38)	3.3
C(A2)	0.35908(29)	0.41659(60)	0.57133(39)	3.4
C(A3)	0.31182(32)	0.52425(56)	0.53822(40)	3.4
Cl(1)	−0.05547(13)	0.22941(26)	0.80384(14)	6.9
Cl(2)	0.08952(12)	0.26915(25)	0.81835(17)	7.8
C(Cl)	0.00568(44)	0.20813(75)	0.75799(48)	5.3
H(S2)	0.0391(30)	0.0420(56)	0.1205(36)	4.0(1.5) [b]
H(S3)	0.0169(34)	0.1316(63)	−0.0122(41)	5.6(1.7) [b]
H(S4)	0.0486(32)	0.3352(60)	−0.0235(38)	4.7(1.6) [b]
H(S5)	0.1010(29)	0.4796(54)	0.1092(34)	3.7(1.4) [b]

Table 10 (continued)

Atom	x	y	z	B_{eq} [a]
H(S6)	0.1137(28)	0.3748(51)	0.2247(33)	3.0(1.3) [b]
H(A11)	0.4182(25)	0.3155(46)	0.6768(30)	2.0(1.1) [b]
H(A12)	0.3626(30)	0.4092(56)	0.6886(35)	3.9(1.4) [b]
H(A2)	0.3855(31)	0.4005(58)	0.5373(36)	4.2(1.5) [b]
H(A31)	0.3222(29)	0.5898(55)	0.5061(34)	3.7(1.4) [b]
H(A32)	0.2961(34)	0.5722(64)	0.5807(40)	5.7(1.7) [b]
H(Cl1)	0.0103(37)	0.1228(70)	0.7413(44)	7.0(2.0) [b]
H(Cl2)	-0.0131(37)	0.2767(70)	0.7071(44)	7.0(2.0) [b]

[a] $B_{eq} = \frac{4}{3}(\Sigma_i \Sigma_j B_{ij} a_i b_j)$ for non-hydrogen atoms. [b] Refined isotropically.

Acknowledgment

The present work was supported by a Grant-in Aid for Scientific Research No. 63106004 from the Ministry of Education, Science and Culture.

References

1 W.L. Gladfelter, K.J. Rosselet, in D.F. Shriver, H.D. Kaesz and R.D. Adams (Eds.), The Chemistry of Metal Cluster Complexes, VCH Publishers, New York, 1990, p. 329; J.P. Fackler, Jr. (Ed.), Metal-Metal Bonds and Cluster in Chemistry and Catalysis, Plenum Press, New York, 1989; B.C. Gates, L. Guczi and H. Knözinger (Eds.), Metal Clusters in Catalysis, Elsevier, Amsterdam, 1986.

2 J.S. Bradley, in F.G.A. Stone and R. West (Eds.), Advances in Organometallic Chemistry, Vol. 22, Academic Press, New York, 1983, p. 1.

3 T. Chihara, K. Aoki and H. Yamazaki, J. Organomet. Chem., 383 (1990) 367.

4 T. Chihara and H. Yamazaki, in preparation.

5 C.T. Hayward and J.R. Shapley, Inorg. Chem., 21 (1982) 3816.

6 B.F.G. Johnson, R.D. Johnson, and J. Lewis, J. Chem. Soc., A, (1968) 2865.

7 D.M.P. Mingos, Acc. Chem. Res., 17 (1984) 311.

8 J.W. Lauher and K. Wald, J. Am. Chem. Soc., 103 (1981) 7648; L.W. Bateman, M. Green, K.A. Mead, R.M. Mills, I.D. Salter, F.G.A. Stone and P. Woodward, J. Chem. Soc., Dalton Trans., (1983) 2599.

9 No reaction was observed without addition of silver tetrafluoroborate. Thallium hexafluorophosphate was used instead of silver hexafluoroborate in the literature: B.F.G. Johnson, D.A. Kaner, J. Lewis, P.R. Raithby and M.J. Taylor, J. Chem. Soc., Chem. Commun., (1982) 314; M.J. Freeman, M. Green, A.G. Orpen, I.D. Slater and F.G.A. Stone, J. Chem. Soc., Chem. Commun., (1983) 2599.

10 G. Lavigne, F. Papageorgiou and J.J. Bonnett, Inorg. Chem., 23 (1984) 609.

11 A. Sirigu, M. Bianchi and E. Benedetti, J. Chem. Soc., Chem. Commun., (1969) 596.

12 G.B. Ansell and J.S. Bradley, Acta Crystallogr., Sect. B, 36 (1980) 726.

13 B.F.G. Johnson, J. Lewis, S.W. Sankey, K. Wong, M. McPartlin and W.J.H. Nelson, J. Organomet. Chem., 191 (1980) C3.

14 P.L. Andreu, J.A. Cabeza, D. Miguel, V. Riera, M.A. Villa and S.G. Granda, J. Chem. Soc., Dalton Trans., (1991) 533.

15 J. Evans, A.C. Street and M. Webster, Organometallics, 6 (1987) 794.

16 B.F.G. Johnson, J. Lewis, N. Nicholls, J. Puga and K.H. Whitmire, J. Chem. Soc., Dalton Trans., (1983) 787.

17 B.F.G. Johnson, J. Lewis, W.J.H. Nelson, J. Puga, P.R. Raithby, D. Braga, M. McPartlin and W. Clegg, J. Organomet. Chem., 243 (1983) C13.

18 S.R. Bunkhall, H.D. Holden, B.F.G. Johnson, J. Lewis, G.N. Pain, P.R. Raithby and M.J. Taylor, J. Chem. Soc., Chem. Commun., (1984) 25.

19 M.I. Bruce and M.L. Williams, J. Organomet. Chem., 288 (1985) C55.

20 C.E. Housecroft, B.F.G. Johnson, J. Lewis, J.A. Lunniss, S.M. Owen and P.R. Raithby, J. Organomet. Chem., 409 (1991) 271.

21 M.I. Bruce, B.K. Nicholson and O.B. Shawkataly, Inorg. Synth., 26 (1989) 324.

22 A.C.T. North, D.C. Phillips and F.S. Mathews, Acta Crystallogr., Sect. A, 24 (1968) 351.

23 (a) D.T. Cromer and J.T. Waber, in J.A. Ibers and W.C. Hamilton (Eds.), International Tables for X-Ray Crystallography, Vol. IV, Kynoch Press, Birmingham, UK, 1974, p. 71; (b) D.T. Cromer, *idem*, p. 148.

24 P. Main, S.E. Hull, L. Lessinger, G. Germain, J.-P. Declerq and M.M. Woolfson, MULTAN78, University of York, York, UK, 1987.

25 T. Sakurai and K. Kobayashi, Rikagaku Kenkyusho Hokoku, 55 (1979) 69.